Journal of the European Ceramic Society 21 (2001) 2311–2317

www.elsevier.com/locate/jeurceramsoc

The effect of doping and processing conditions on properties of $La_{1-x}Sr_xGa_{1-y}Mg_yO_{3-\alpha}$

V.P. Gorelov [a], D.I. Bronin [a,*], Ju. V. Sokolova [a], H. Näfe [b], F. Aldinger [b]

[a] *Institute of High-Temperature Electrochemistry, S. Kovalevskaja, 20 620219 Ekaterinburg, Russia*
[b] *Max-Planck-Institut für Metallforschung, Pulvermetallurgisches Laboratorium, Heisenbergstr. 5, D-70569 Stuttgart, Germany*

Received 31 March 2000; received in revised form 4 December 2000; accepted 2 January 2001

Abstract

The phase composition and electrical conductivity of ceramics based on $La_{1-x}Sr_xGa_{1-y}Mg_yO_{3-\alpha}$ (LSGM) were studied after doping with different quantities of Sr and Mg. The effect of the processing conditions on the density of the LSGM ceramics was analysed. By means of microprobe X-ray analysis it was found that the limit solubility of Sr and Mg in $LaGaO_3$ corresponded to $x=y\approx 0.16$. If excess Sr and/or Mg is added, $LaSrGa_3O_7$ and/or $La_4Ga_2O_9$ phases are formed respectively in addition to the main $LaGaO_3$ perovskite phase. No other impurity phases were detected. The maximum electrical conductivity of LSGM was achieved in the region of the limit solubility of the dopants.

Keywords: Electrical conductivity; Inclusions; (La, Sr) (Ga, Mg)O_3; Perovskites; X-ray methods

1. Introduction

Today a lot of investigations are aimed at decreasing the working temperature of SOFCs and other electrochemical devices with solid oxide electrolytes. In this connection, researchers look for and examine high-conductivity solid oxide electrolytes that can be used in electrochemical devices instead of traditional ZrO_2-based electrolytes which have a relatively low electric conductivity.

A promising material is the solid electrolyte based on $LaGaO_3$ perovskite, which is doped with strontium in the lanthanum sublattice and with magnesium in the gallium sublattice: $La_{1-x}Sr_xGa_{1-y}Mg_yO_{3-\alpha}$ (LSGM).[1] Its conductivity is higher than that of Y_2O_3- or Sc_2O_3-doped ZrO_2 and is comparable with the conductivity of Gd_2O_3-doped CeO_2. However, CeO_2-based solid electrolytes have a narrow electrolytic range and have high proportion of electronic conductivity even in weakly reducing atmospheres. Solid LSGM electrolytes are devoid of this drawback. Their ionic transfer number is close to unity over a broad range of oxygen activity in the gaseous phase.[2]

High conductivity values are typical of LSGM when Sr and Mg concentrations range between 10 and 20 at.% of the concentration of the substituted cations (La and Ga, respectively). Concentrations of the Sr and Mg additions are not necessarily equivalent, the concentration of one component may exceed the concentration of the other.[1,3,4]

The single-phase LSGM ceramic proved to be difficult to synthesise. Some papers dedicated to synthesis and study of this electrolyte report the presence of traces of second phases (or phase).[5,6] Considering that ''traces'' means the amounts detected by the X-ray phase analysis, and that the sensitivity threshold of this method can be 3–4%, the phase diversity of LSGM may be high. Taking LSGM 10–20 (the numerals denote percentage of Sr and Mg respectively) as an example, it was shown[7] that synthesis conditions can considerably affect the ceramic phase composition.

The present work deals with the study of the phase composition and electrical conductivity of $La_{1-x}Sr_xGa_{1-y}Mg_yO_{3-\alpha}$, as a function of doping. The effect of processing conditions on the density of the LSGM 20-15 ceramic was analysed.

* Corresponding author. Tel.: +007-3432-493062.
E-mail address: bronin@ihte.uran.ru (D.I. Bronin).

0955-2219/01/$ - see front matter
PII: S0955-2219(01)00203-5

2. Experimental

2.1. Preparation of the samples

Differently doped LSGM samples were prepared using the starting materials given in the Table 1. To prepare samples of LSGM the required amounts of the starting powders were ground with alcohol in an agate mortar. The mixture was dried and then calcined as a powder. The calcined powder was ground again and samples were prepared by pressing under isostatic conditions at 625 MPa and sintering. Calcination and sintering alike were carried out in air in a closed alumina crucible. The temperature and the duration of both calcination and sintering for the sample tested are given in Table 2 and in the relevant sections of the paper.

The influence of processing conditions on the phase composition and density of the ceramics was examined using the example of LSGM 20-15. Once prepared, the mixture of starting materials was used in all the experiments on LSGM 20-15 ceramic.

2.2. Density

The sintered samples were characterised for density using the Archimedes method in deionised water. The relative densities of different LSGM samples were estimated with reference to the theoretical density of 6.68 g/cm^3, which was calculated from the parameters of the LSGM 10-20 elementary cell.[4]

Table 1
Starting materials used in the preparation of LSGM ceramics

Batches	Samples	Raw products (% chemical purity) and supplier
I	LSGM 5-5	La_2O_3 (99.9) PFCR, USSR
	LSGM 10-10	Ga_2O_3 (99.5) Red Chemists, USSR
	LSGM 15-15 (I)	$SrCO_3$ (99.999) Red Chemists, USSR
	LSGM 20-20	$(MgCO_3)_4{\cdot}Mg(OH)_2{\cdot}5H_2O$ (99.999) Red Chemists, USSR
II	LSGM 10-20	La_2O_3 (99.99) Aldrich
	LSGM 15-15 (II)	Ga_2O_3 (99.999) Alfa
	LSGM 20-15	$SrCO_3$ (99.994) Alfa
	LSGM 12-18	$(MgCO_3)_4{\cdot}Mg(OH)_2{\cdot}5H_2O$ (99.99) Alfa

2.3. Phase composition

The phase composition of the LSGM samples was examined using SEM and X-ray microanalysis. X-ray diffraction analysis was not used, some of additional diffraction lines, which belong to the minor phases, are interpreted ambiguously in the literature. No analysis was done to examine whether the chemical reaction between the raw products was completed during precalcination or whether it continued during sintering. The ceramics were only analysed after the final sintering.

2.4. Electrical conductivity measurements

The conductivity of the samples from the batch I (Table 1) was determined in the temperature region 613–1023°C by the square-pulse method using a bridge circuit assembled from a pulse generator, an oscilloscope, and a resistance box. The conductivity measurements with the samples from the batch II (Table 1) were performed by impedance method over the frequency range of 1–10^6 Hz using an impedance-meter (IM 5d Zahner-electrik) at temperatures ranging from 439–861°C. The samples were shaped as rectangular bars with the length/cross-sectional area ratio of 5–14 cm^{-1}. The electrodes were made from a fine platinum powder attached to the electrolyte and fired at 950°C for 1 h.

2.5. DTA and dilatometry

Heat effects studies were carried out with the sintered materials by a device for thermal and gravimetric analysis (STA 501, Bähr) starting with room temperature and ending at 1600°C at the rate of 2°C/min. The mass of the probe was approximately about 0.5 g. The high-temperature dilatometer (Theta Indust. Co., USA) was used to study the shrinkage phenomena of the precalcined pressed samples during heating.

Table 2
Secondary phases found in differently doped LSGM ceramics prepared under corresponding processing conditions

Composition	Calcination and sintering temperatures (time)	Secondary phases
LSGM 5-5	1200°C (1 h), 1450°C (1.5 h)	Traces of $LaSrGa_3O_7$ and $La_4Ga_2O_9$
LSGM 10-10	1200°C (1 h), 1450°C (1.5 h)	Traces of $LaSrGa_3O_7$ and $La_4Ga_2O_9$
LSGM 15-15	1200°C (1 h), 1450°C (1.5 h)	Traces of $LaSrGa_3O_7$
LSGM 20-20	1200°C (1 h), 1450°C (1.5 h)	$LaSrGa_3O_7$ and $La_4Ga_2O_9$
LSGM 10-20	1420°C (10 h)	$La_4Ga_2O_9$
LSGM 20-15	1100°C (1 h), 1520°C (10 h)	$LaSrGa_3O_7$
	1300°C (1 h), 1520°C (10 h)	$LaSrGa_3O_7$
	1520°C (1 h), 1520°C (6 h)	$LaSrGa_3O_7$

3. Results and discussion

3.1. Micro-probe X-ray analysis of differently doped LSGM

SEM showed that all the examined samples contained at least a small quantity of the secondary phase(s). The compositions of these phases determined by X-ray microanalysis are presented in the Table 2. The phase $LaSrGa_3O_7$ appeared in the SEM pictures as darker grains and the $La_4Ga_2O_9$ grains were lighter than the main matrix of the samples (Fig. 1a–e).

The X-ray microanalysis method was also used to examine the composition of the main $LaGaO_3$ phase (matrix) of different LSGM samples. Fig. 2 shows the dependence of Sr and Mg content in the matrix of LSGM (vertical co-ordinates) on the nominal quantity of Sr and Mg in the starting product (horizontal co-ordinates, where x and y denote the corresponding values of Sr and Mg, respectively, in the substance of nominal composition $La_{1-x}Sr_xGa_{1-y}Mg_yO_{3-\alpha}$). The analysis showed that the concentration of Sr and Mg in the matrix of LSGM samples corresponds to the introduced amount of the dopants only up to the values of x and y less then about 0.16. At higher doping the dependence attains saturation. This means that the samples with x and $y < 0.16$ belong to single-phase $LaGaO_3$-based solid solutions. The presence of minor inclusions of secondary phases in $LaGaO_3$ doped with low content of Sr and Mg (x, $y < 0.16$) can possibly be attributed to secondary causes, such as inhomogeneity of the mixture of initial components despite careful grinding before and after pre-calcination and/or only slight difference between the energy of formation of the main $LaGaO_3$ phase and of an impurity phase.

The solubility limit of each dopant does not depend on the concentration of the other dissolved in $LaGaO_3$. It is seen from Fig. 2 that the concentrations of Sr and Mg in the matrices of the LSGM 20-15 and LSGM 10-20, respectively, correspond to the same solubility limits for samples doped with equal amount of Sr and Mg.

Only the second dark phase corresponding to $LaSrGa_3O_7$ was present in the LSGM 20-15 sample (Fig. 1a–c) and only the light phase of $La_4Ga_2O_9$ was observed in the LSGM 10-20 sample (Fig. 1d). Both of these phases were present in LSGM 20-20 (Fig 1e). These facts are in complete agreement with the found value of limit solubility of Sr and Mg in $LaGaO_3$. No other secondary phases were detected in our study in any of the LSGM samples produced under different processing conditions.

3.2. The effect of processing conditions on density of LSGM ceramic

This part of the study was carried out using electrolyte of composition LSGM 20-15 as an example with the aim of finding processing conditions which enable to produce high density LSGM ceramic. The very first experiments showed that the porosity of the LSGM was strongly determined by the rate of heating at different sections of the whole temperature range during sintering of compact samples pressed from preliminary calcined and milled powders. The extent of porosity could not be significantly decreased by means of only higher temperatures or longer periods of sintering. The dilatometric examination taken in the course of heating (5°C/min) of compact sample prepared from calcined at 1100°C (1 h) and then ground powder of LSGM, Fig. 3, showed that the sintering itself started at about 900°C. At this temperature the heating rate should be decreased or the heating ramp should be stopped to preclude formation of pores due to entrapment of gases released from the sample. Within the lower temperature range 250–700°C the length of the sample was almost independent of the temperature. This fact can be explained by the decomposition of some products of interaction of the material with atmospheric water and/or carbon dioxide which arose during the preparation of compact sample from powder and/or in the course of the heating the sample from room temperature to 200–250°C. It was absolutely necessary to protect the pre-calcined materials from their interaction with the surrounded air before sintering. After 10–20 h of their storage in air at room temperature considerable increase in the volume of not sintered samples was seen even visually.

The further experiments revealed that density of the samples decreased with increasing pre-calcination temperature of the initial mixture. Thus the samples pre-calcined at 1100 and 1400°C and sintered at 1300°C (1 h) had the density of 5.38 g/cm^3 (81% of the theoretical value) and 4.68 g/cm^3 (70%), respectively. Even when the sintering lasted at 1420°C for 15 h, the samples still had considerably different density values: 6.34 g/cm^3 (95%) and 5.95 g/cm^3 (89%), respectively. The loss of sinterability when increasing the calcination temperature of starting materials is well known among the ceramists. The effect of the pre-calcination temperature on the ceramic density decreased progressively as the sintering temperature was raised, and diminished almost completely at the sintering temperature of 1520°C. Indeed, when the aforementioned samples were sintered at 1520°C (10 h), their density values became 6.52 g/cm^3 (98%) and 6.48 g/cm^2 (97%), respectively. This behaviour can be understood when the results of the DTA experiment performed within the interval from room temperature to 1600°C are considered (Fig. 4): the sample fused and the DTA curve exhibited an endo-effect in the region of 1574°C during heating (the other peaks seen in Fig. 4 at 1445 and 1600°C are artificial apparatus effects manifesting themselves when any change in heating and cooling ramps as well as at transition from heating to cooling took place). This temperature point should fall on the solidus line in the

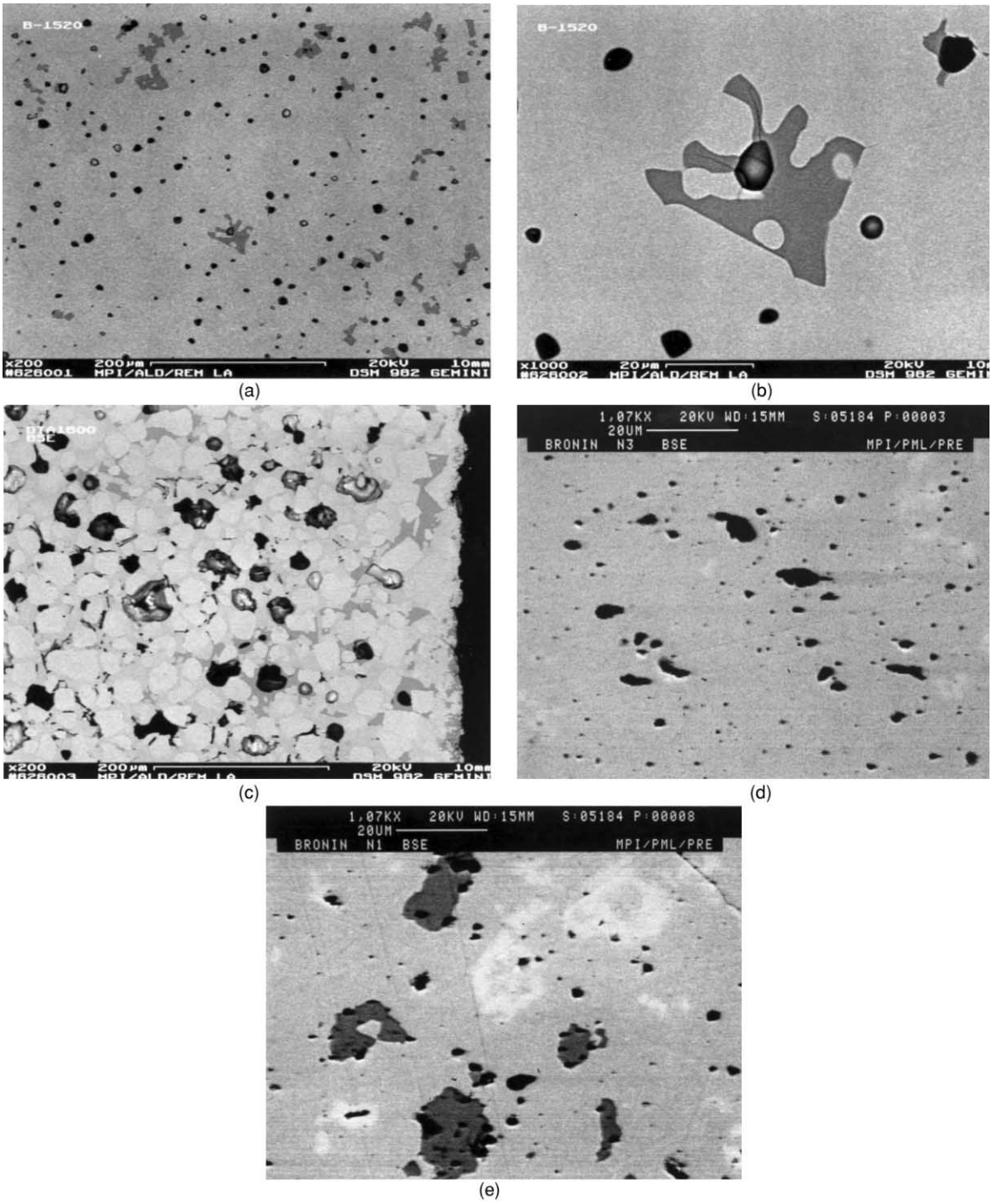

Fig. 1. SEM micrographs of LSGM electrolyte (light inclusions, $La_4Ga_2O_9$; grey inclusions, $LaSrGa_3O_7$; black spots, pores): (a) LSGM 20-15, sintered at 1520°C (×200); (b) LSGM 20-15, sintered at 1520°C (×1000); (c) LSGM 20-15 after melting (×200); (d) LSGM 10-20, sintered at 1420°C (×1000); (e) LSGM 20-20, sintered at 1450°C (×1000).

phase diagram of LSGM. Thus, at the sintering temperature of 1520°C the samples are at or near to the pre-melting stage, when the diffusion coefficient of ions is high and the method of sample preparation is no longer important.

Since in the DTA experiment the sample was melted in a crucible of aluminium oxide, it was interesting to determine the mutual diffusion depth of aluminium and LSGM 20-15 cations at the melt interface, especially as aluminium and gallium are chemical analogues. The time of contact between the melt and the crucible at temperatures from 1574–1600°C was 22 min. However, the microprobe analysis did not detect any mutual diffusion of cations between LSGM and alumina within the analytical error.

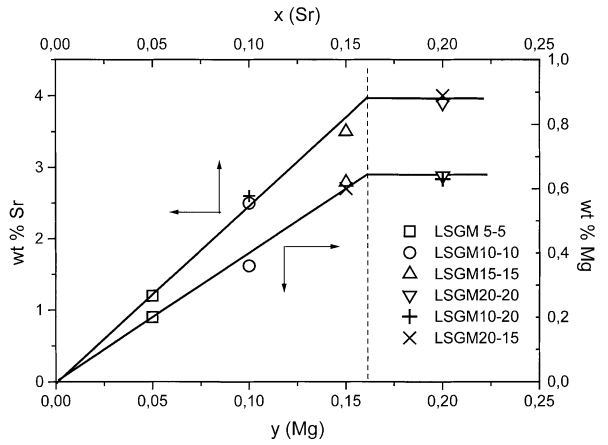

Fig. 2. Concentration of Sr and Mg in the matrix of differently doped LSGM samples. Vertical co-ordinates, content of Sr and Mg in the matrix of LSGM found by X-ray microanalysis; horizontal co-ordinates, quantity of Sr and Mg in the starting products corresponding to x and y, respectively, in the substance of nominal composition $La_{1-x}Sr_xGa_{1-y}Mg_yO_{3-\alpha}$.

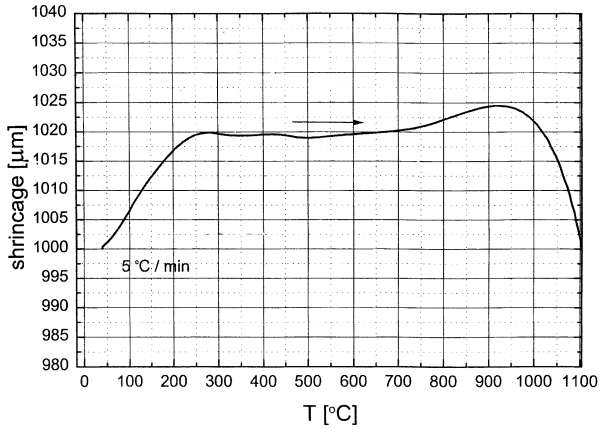

Fig. 3. Dilatometric curve taken on the sample LSGM 20-15 prepared from the powder calcined at 1150°C (1 h).

The analysis of the LSGM 20-15 ceramic suggests that processing conditions: the pre-calcination temperature (1100–1520°C), number of calcinations (1–3) with intermediate grinding, the state of the calcined mixture (compacts or powder), the sintering temperature (1400–1520°C) and duration of the sintering (2–15 h), have a minor influence on the phase composition of the samples. All the samples of LSGM 20-15 contained the secondary phase in addition to the main $LaGaO_3$ phase. According to the X-ray microanalysis, the second phase corresponded to $LaSrGa_3O_7$ (Fig. 1a–c). It is noteworthy that the $LaSrGa_3O_7$ phase poorly dissolves magnesium and its magnesium concentration does not exceed 0.3–0.5 at.%. As a result of the present study, the samples having a density of 96–99% of the theoretical value were successfully produced under sintering conditions which prevented the interaction between the pre-

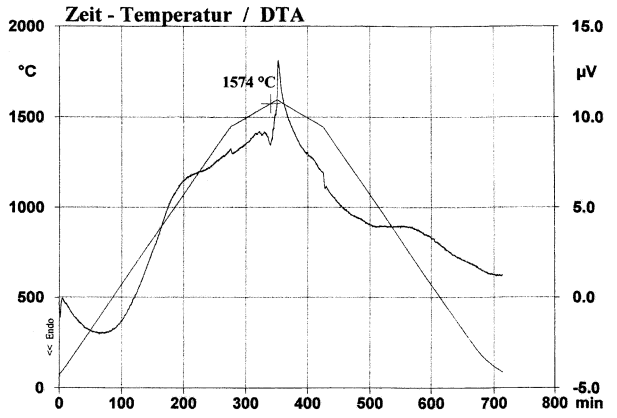

Fig. 4. DTA curve taken on the sample LSGM 20-15 sintered at 1520°C (12 h).

calcined sample with the gas phase and obstructed the formation of pores. The following procedure of sintering in order to produce dense LSGM was employed: heating up to 900°C (8–9°C/min), exposure at 900°C (0.5 h), heating up to 1400–1500°C (2°C/min), exposure at 1400–1500°C (10–12 h), and cooling down to room temperature (5°C/min). Considering the density of the samples obtained under the above procedure as sufficiently high we did not attempt further to increase in the samples density.

3.3. Electrical conductivity

The dependence of the electrical conductivity as a function of doping taken at different temperatures is depicted in Fig. 5. When $LaGaO_3$ was doped with equal amounts of strontium and magnesium at the step $x=y=0.05$, electrical conductivity of LSGM increased with doping, up to its maximum value at $x=y=0.15$. The next composition with $x=y=0.20$ had much lower conductivity and the sample was not monophasic (Fig. 1e). The $LaSrGa_3O_7$ (dark) and $La_4Ga_2O_9$ (light) phases were present in large quantities. Thus, the maximum electrical conductivity of this system corresponds to the region of saturation limits of Sr and Mg in LSGM.

It should be particularly emphasised that in such well studied systems as doped zirconia and ceria the electrical conductivity accordingly increases with increasing the concentration of aliovalent guest cations at the initial stage of doping. Further substitution of more than 8–10% of host cations leads to progressive decrease in the electrical conductivity even in the region of monophasic solid solutions.[8,9] This phenomenon is often explained as a result of the formation of neutral defect cation-vacancy pairs or by ordering of vacancies in the anion sublattice. In contrast, in the LSGM system the electrical conductivity peaks at substitution of 30–35% of corresponding sites and in the region where the secondary phase(s) appear(s). This behaviour is, probably, indica-

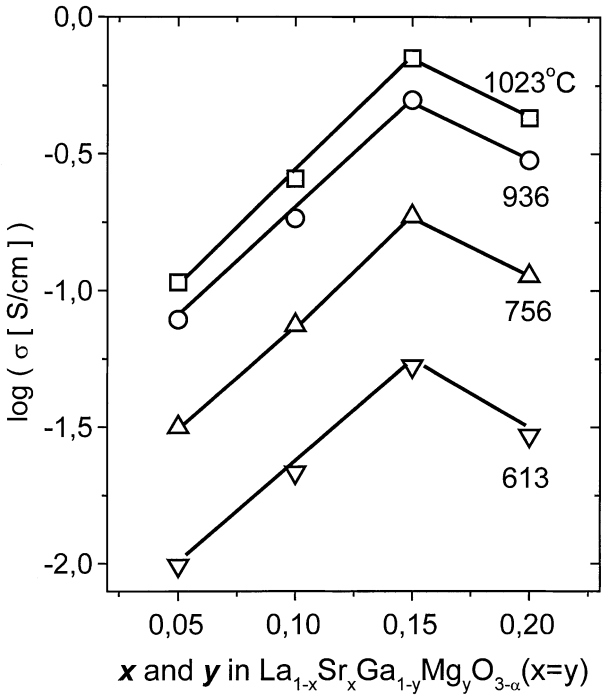

Fig. 5. Electrical conductivity of $La_{1-x}Sr_xGa_{1-y}Mg_yO_{3-\alpha}$ at different temperatures as a function of doping with equal quantities of Sr and Mg ($x=y$).

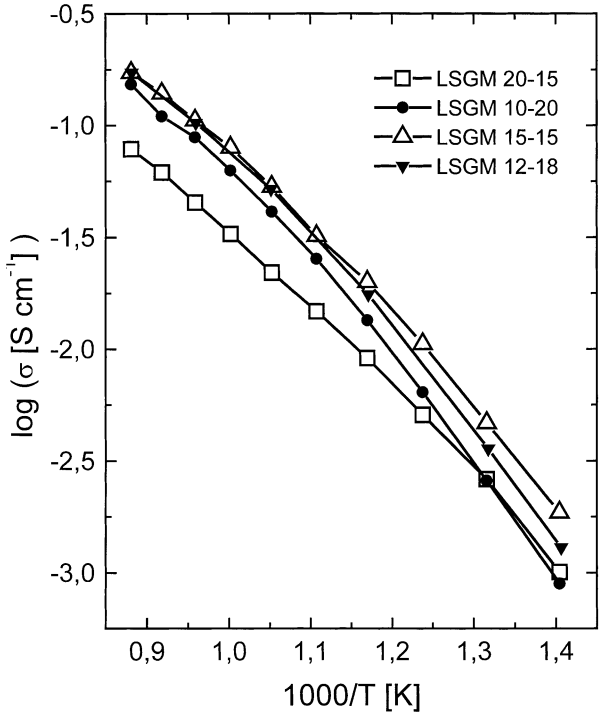

Fig. 7. Arrhenius plot of electrical conductivity for the best conducting LSGM electrolytes.

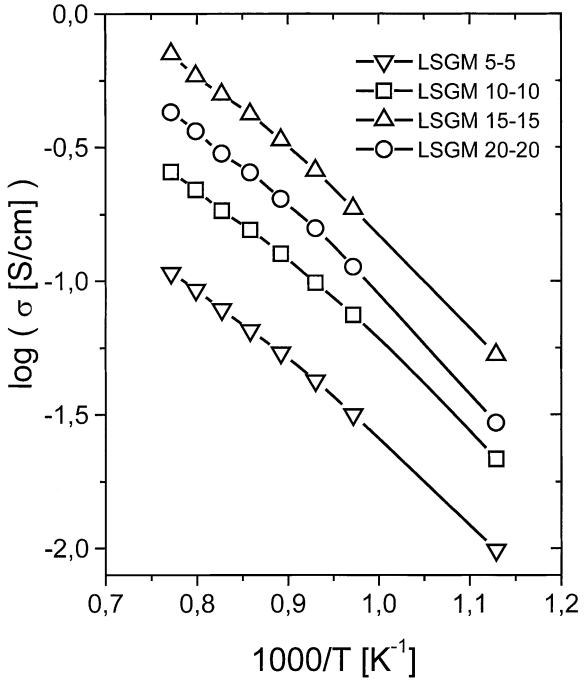

Fig. 6. Temperature dependence of electrical conductivity of LSGM samples differently doped with equal quantities of Sr and Mg ($x=y$).

tive of the inapplicability of the point defects model to LSGM system for the description of ionic transfer.

The temperature vs. electrical conductivity curves plotted for the LSGM samples in the Arrhenius coordinates show that the electrical conductivity activation energy rises with decreasing temperature (Figs. 6 and 7), similar to ZrO_2-based electrolytes. Electrical conductivity values of the LSGM 15-15, LSGM 12-18 and LSGM 10-20 samples differ little and slightly exceed the electrical conductivity value of LSGM 20-15 sample (Fig. 7). The results obtained in the present study correspond well to the opinion of previous studies[10] that for $La_{1-x}Sr_xGa_{1-y}Mg_yO_{3-\alpha}$ the highest conductivity usually occurs at $x+y=0.35$.

4. Conclusions

The phase composition and electrical conductivity of LSGM solid solutions doped with Sr and Mg were examined. The Sr and Mg solubility limit was found to be at $x=y\approx0.16$ for the formula $La_{1-x}Sr_xGa_{1-y}Mg_yO_3$. If excess Sr and/or Mg was added to the main $LaGaO_3$ phase, $LaSrGa_3O_7$ and/or $La_4Ga_2O_9$ phases were formed in addition to the main $LaGaO_3$ perovskite phase. Processing conditions that affect synthesis of dense (96–99% of the theoretical value) LSGM ceramics were analysed. The temperature dependence of electrical conductivity of the LSGM solid electrolytes was studied as a function of doping with strontium and magnesium. The maximum electrical conductivity was achieved in the region of the limit solubility of the dopants.

Acknowledgements

The authors thank F.M. Keppeler (Max-Planck-Institut für Metallforschung, Department Aldinger, Stuttgart) for assistance during the course of these studies. This work was carried out within the Project RUS-137-97 financially supported by Bundesministerium für Bildung, Wissenschaft, Forschung und Technologie, Germany.

References

1. Ishihara, T., Matsuda, H. and Takita, Y., Doped $LaGaO_3$ perovskite type oxide as a new oxide ionic conductor. *J. Am. Chem. Soc.*, 1994, **116**, 3801–3803.
2. Stevenson, J. W., Armstrong, T. R., McCready, D. E., Pederson, L. R. and Weber, W. J., Processing and electrical properties of alkaline earth-doped lanthanum gallate. *J. Electrochem. Soc.*, 1997, **144**, 3613–3620.
3. Petric, A., Huang, P. and Skowron, A. Characterization of the conductivity and structure of lanthanide gallate perovskites. In *Proceedings of the 2nd European SOFC Forum*, Vol. 2, ed. B. Thorstensen. Switzerland, 1996, pp. 751-760.
4. Slater, P. R., Irvin, J. T. S., Ishihara, T. and Takita, Y., The structure of the oxide ion conductor $La_{0.9}Sr_{0.1}Ga_{0.8}Mg_{0.2}O_{2.85}$ by powder neutron diffraction. *Solid State Ionics*, 1998, **107**, 319–323.
5. Ishihara, T., Matsuda, H. and Takita, Y., Doped $LaGaO_3$ perovskite type oxide as a new oxide ionic conductor. In *Ionic and Mixed Conducting Ceramics*, ed. T. A. Ramanarayanan, W. L. Worrel and H. L. Tuller. The Electrochem. Soc. Proc. Series, PV 94-12, Pennington, New York, 1994, pp. 85–93.
6. Stevenson, J. W., Armstrong, T. R., Pederson, L. R., Li, J., Lewinsohn, C. A. and Baskaran, S., Effect of A-site cation non-stoichiometry on the properties of doped lanthanum gallate. *Solid State Ionics*, 1998, **113-115**, 571–583.
7. Djurado, E. and Labeau, M., Second phases in doped lanthanum gallate perovskites. *J. Eur. Ceram. Soc.*, 1998, **18**, 1397–1404.
8. Etsell, T. H. and Flengas, S. N., The electrical properties of solid oxide electrolytes. *Chem. Rev.*, 1970, **70**, 339–376.
9. Gorelov, V. P. and Palguev, S. F., Electrical conductivity maximum and boundary of fruorite-type phase in ZrO_2-rare earth element systems. *Doklady AN SSSR*, 1979, **248**, 1356–1359 (in Russian).
10. Huang, P. and Petric, A., Superior oxygen ion conductivity of lanthanum gallate doped with strontium and magnesium. *J. Electrochem. Soc.*, 1996, **143**, 1644–1648.